

Microstructures and mechanical properties of MgAl₂O₄ particle-reinforced AC4C aluminum composites

Tateoki IIZUKA¹, Qiu-bao OUYANG²

1. Isuzu Advanced Engineering Center, Ltd., Kanagawa 252-0881, Japan;

2. State Key Laboratory of Metal Matrix Composites, Shanghai Jiao Tong University, Shanghai 200240, China

Received 17 October 2013; accepted 8 April 2014

Abstract: MgAl₂O₄ particle-reinforced AC4C based alloy composites were fabricated by the stirring–casting method. The effects of the average sizes and the size distributions of MgAl₂O₄ particles on the dispersibility were investigated, and the microstructures, strength, and fatigue properties of MgAl₂O₄ particle-reinforced AC4C based alloy composites were evaluated. Tensile strength in the MgAl₂O₄ particle-reinforced AC4C based alloy composite was increased by using the classified particles. The fatigue limit at 10⁷ cycles in the MgAl₂O₄ particle-reinforced AC4C-Cu composite increased by 27% compared to the unreinforced alloy at 250 °C. Dislocations were observed in the matrix around the MgAl₂O₄ particle which resulted from the mismatch of thermal expansion coefficients between MgAl₂O₄ and Al, and resisted failure and caused fatigue cracks to propagate around the MgAl₂O₄ particles, resulting in extensive crack deflection and crack bowing, which contributed to the improvement of fatigue strength.

Key words: MgAl₂O₄ particle; AC4C based aluminum alloy; classification of particles; composite; fatigue; tensile strength

1 Introduction

Because ceramic particle-reinforced aluminum matrix composite has excellent strength at elevated temperatures, high specific modulus and wear resistance, it is promising for automobile and aerospace applications. Among the ceramic particles, SiC and Al₂O₃ particles are mostly used in particle-reinforced aluminum composites, and the stirring-casting method is the most inexpensive process for fabricating the composites. However, SiC particles can react with Al to generate Al₄C₃ particles on the surfaces even in solid state when no Si is present originally in the Al alloy [1–4]. To avoid reaction between SiC and the molten aluminum alloy, the concentration of Si in the alloy must be higher than a certain critical value [4]. Moreover, when the Al₂O₃ particles are incorporating into the Mg-containing molten aluminum alloy, magnesium aluminate spinel (MgAl₂O₄) particles generate on the surfaces of Al₂O₃ particles [5–7]. In general, in order to improve the dispersibility and wettability of SiC particles with the molten aluminum, the oxidation treatment of SiC particles at a temperature higher than 900 °C is required to form a thin

layer of SiO₂ amorphous on the surfaces of SiC particles. The thin amorphous SiO₂ layer can react with Mg and Al to generate the MgAl₂O₄ particles on the surfaces of SiC particles when the oxidized SiC particles are dispersed into the Mg-containing molten aluminum alloy [8–10]. The reaction between the aluminum alloy and the particles becomes violent when the Mg-containing molten aluminum alloy is held at a high temperature status for a long period of time, and Mg content is gradually consumed during the reaction. In the aluminum alloys, because Mg contributes to the generation of Mg₂Si resulting in the improvement of the strength, the decrease in the content of Mg can cause decreased strength. However, controlling the content of Mg in aluminum alloys is very difficult due to the reaction between the particles and molten aluminum alloys for SiC and Al₂O₃ particles reinforced Mg-containing aluminum alloys. In order to prevent violent reaction, the temperature of the molten aluminum alloy dispersed with Al₂O₃ particles or SiC particles is required not to exceed 750 °C. Therefore, ceramic particles which can be chemically stable dispersed in molten aluminum alloys even at high temperatures are desired.

In view of the above, MgAl₂O₄ particles have been

used as reinforcement in the present study due to MgAl_2O_4 being the final reaction product for above mentioned reaction. The MgAl_2O_4 particles do not react with Mg-containing molten aluminum alloy and can be present in the molten aluminum alloy stably. MgAl_2O_4 particle reinforced AC4C based alloy composites were prepared by the melt-stirring method, and the specimens were cast by the gravity casting. For evaluating the dispersibility of MgAl_2O_4 particles in molten aluminum alloys, the effects of the average sizes and the size distributions of MgAl_2O_4 particles were investigated. The microstructures, strength, and fatigue properties of MgAl_2O_4 particle-reinforced AC4C based alloy composites were also evaluated.

2 Experimental

Two types of MgAl_2O_4 particles were used as reinforcements in this study, and the average particle sizes of as-received MgAl_2O_4 particles were 2.5 μm and 12.2 μm , respectively. Because the as-received MgAl_2O_4 particles were not classified as abrasives such as with SiC particles, the particle sizes were distributed over a wide range. The size distribution of as-received MgAl_2O_4 particles with an average particle size of 12.2 μm is shown in Fig. 1(a), and the particle sizes distribute in a range of 0.4–90 μm . Due to the dispersion of fine particles to molten aluminum alloy being very difficult, the as-received MgAl_2O_4 particles with an average size of 12.2 μm were classified. During the classification of MgAl_2O_4 particles, the particles with a size in a range of 5–25 μm were collected. The size distribution of classified MgAl_2O_4 particles is shown in Fig. 1(b), and the average particle size is 9.6 μm .

MgAl_2O_4 particle-reinforced AC4C (Al–7%Si–0.4%Mg, mass fraction) based alloy composites were fabricated by the melt stirring–gravity casting method. Before the particles were added to a molten aluminum alloy, MgAl_2O_4 particles were preheated at 1000 $^\circ\text{C}$ to remove the moisture adhered to the particles, and 0.3% of magnesium was added to AC4C alloy (defined as AC4C–Mg:Al–7%Si–0.7%Mg) to improve the dispersibility of MgAl_2O_4 particles. For evaluating the effect of composition of the matrix alloy on the mechanical properties of the composite, 1% copper was added to AC4C–Mg alloy (defined as AC4C–Cu:Al–7%Si–0.6%Mg–1%Cu). 10% heat-treated MgAl_2O_4 particle was then added into the molten AC4C–Mg and AC4C–Cu alloys through the vortex. Finally, the melt was poured into a mould with dimensions of 200 mm \times 40 mm \times 30 mm. After solidification, the resulting composites were removed from the mould and subjected to a T6 heat-treatment. The microstructures of the obtained composites were characterized by optical

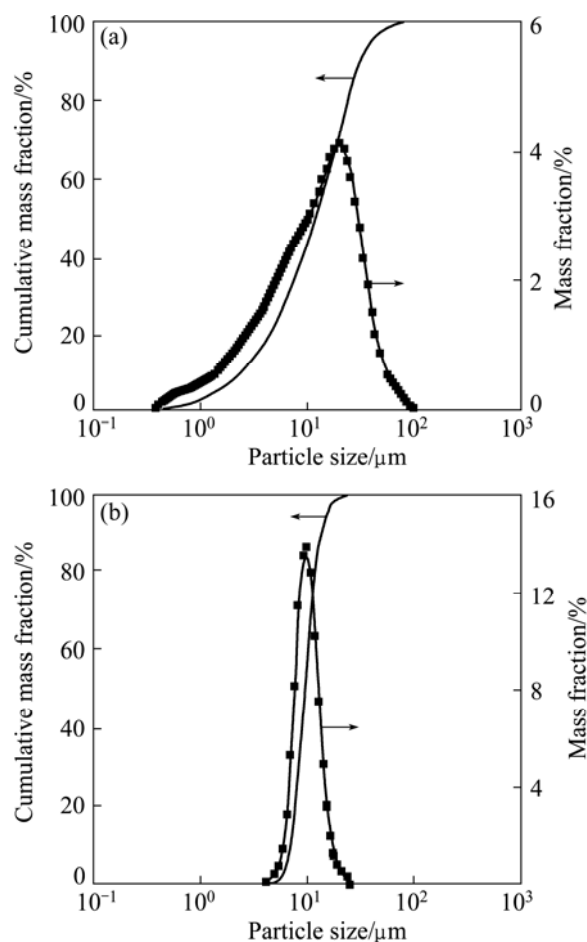


Fig. 1 Particle distributions: (a) As-received particles with average size of 12.2 μm ; (b) Classified particles with average size of 9.6 μm

microscopy and transmission electron microscopy (TEM). For optical observations, the heat-treated materials were cut and polished. TEM specimens were prepared by cutting, mechanical grinding, dimpling, and ion thinning. For measuring the tensile strength, the materials were machined to tensile strength specimens with a gauge length of 30 mm and a diameter of 6 mm. The tensile strength tests were conducted at room temperature, and the displacement rate was 2 mm/min. The fatigue tests were conducted under load control using a rotation bending fatigue machine at room temperature and 250 $^\circ\text{C}$. The frequency of sinusoidal waves was 50 Hz with a stress ratio of -1 . The specimens for fatigue tests had a gauge length of 10 mm and a diameter of 8 mm. Fatigue tests were terminated at complete separation of the specimen or after 10^7 cycles were accumulated. Tensile and fatigue data of the composites were compared with the data of un-reinforced matrix alloy. The fracture surfaces of fatigue specimens were observed by an optical microscope and scanning electronic microscope (SEM).

3 Results and discussion

3.1 Effect of particle size and distribution on dispersibility

The microstructures of MgAl_2O_4 particles-reinforced AC4C based alloy composites are shown in Fig. 2. When the average particle size of MgAl_2O_4 was $2.5\ \mu\text{m}$, particle agglomeration occurred during the dispersion process, and a lot of defects caused by the agglomeration were present in the composite. When the average particle size was $12.2\ \mu\text{m}$ and particles were not classified (Fig. 2(b)), the coarse particles and the fine particles co-existed in the composite. The fine particles were aggregated in places, and many of fine particles gathered in the vicinity of the coarse particles. It was found that the particle agglomerations became intense when the particle size was below $3\ \mu\text{m}$, but the particles were individually dispersed gradually when particle size was $3\ \mu\text{m}$ and above. When the particle size reached more than $5\ \mu\text{m}$, almost no particle agglomeration existed in the composite. Therefore, in order to improve the dispersibility of the particles and the strength of composite, the as-received MgAl_2O_4 particles with an average particle size of $12.2\ \mu\text{m}$ were classified by excluding the fine particles and the coarse particles, and the particles with a size in a range of $5\text{--}25\ \mu\text{m}$ were collected and used for fabricating the composite.

Figures 2(c) and 2(d) show the microstructures of the classified MgAl_2O_4 particle reinforced AC4C–Cu alloy composite. The classified particles were uniformly distributed in the matrix, and the agglomerations of the particles were not observed.

3.2 Microstructures

Because AC4C–Mg and AC4C–Cu alloys are the Al–Si based hypoeutectic aluminum alloys, the main phases of $\text{MgAl}_2\text{O}_4/\text{AC4C–Mg}$ and $\text{MgAl}_2\text{O}_4/\text{AC4C–Cu}$ composites are primary $\alpha(\text{Al})$, eutectic structures and MgAl_2O_4 particles as shown in Fig. 2. Primary $\alpha(\text{Al})$ phases grew up as the dendrite, and the MgAl_2O_4 particles were distributed in the eutectic regions of the grain boundaries of primary $\alpha(\text{Al})$ phases. However, the MgAl_2O_4 particles showed a strong tendency to accumulate in clusters which existed in the last stage of solidification while the size of the particles was below $3\ \mu\text{m}$ as shown in Fig. 2(a). Si phases were seen apparently in the eutectic regions, and some Si phases emerged from the surfaces of the MgAl_2O_4 particles.

Figure 3 shows the TEM micrographs of the classified $\text{MgAl}_2\text{O}_4/\text{AC4C–Cu}$ composite. The MgAl_2O_4 particle exhibited perfect interface with the Al matrix, and the $\text{MgAl}_2\text{O}_4/\text{Al}$ interface was clean and free of secondary phases. The natural surface of MgAl_2O_4 particle was (111) plane with a lattice-fringe spacing of $0.47\ \text{nm}$. Because the MgAl_2O_4 particles were

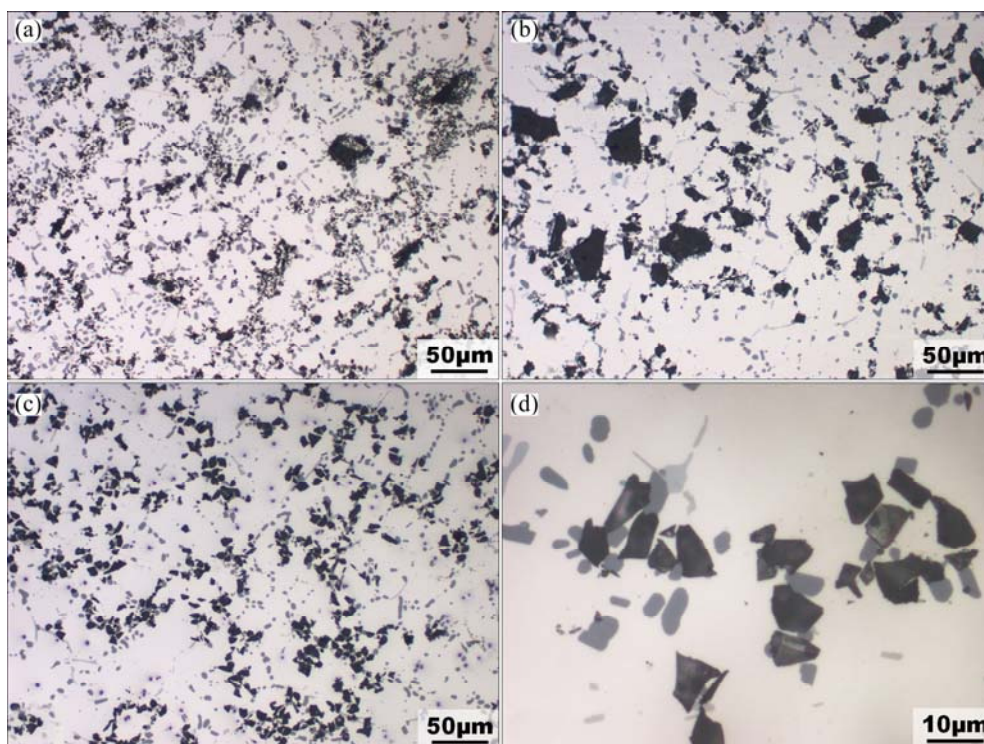


Fig. 2 Optical micrographs of $\text{MgAl}_2\text{O}_4/\text{AC4C}$ based alloy composites: (a) As-received particles (average size of $2.5\ \mu\text{m}$)/AC4C–Mg composite; (b) As-received particles (average size of $12.2\ \mu\text{m}$)/AC4C–Mg composite; (c), (d) Classified particles (average size of $9.6\ \mu\text{m}$)/AC4C–Cu composite

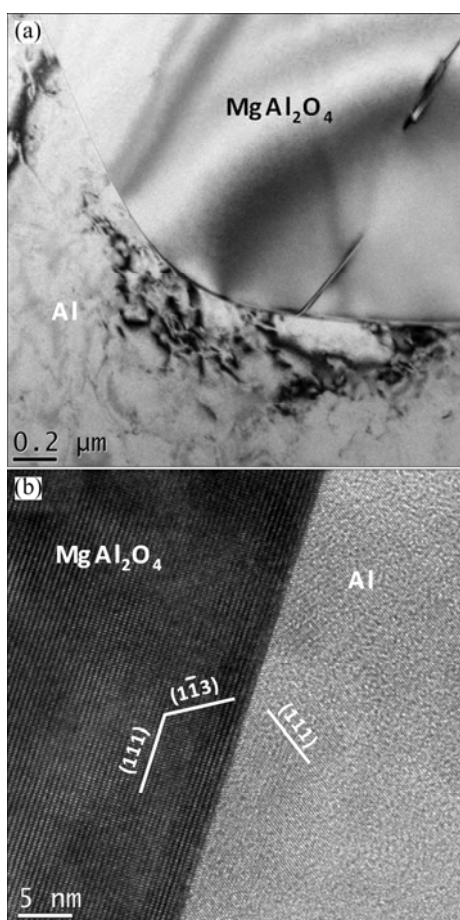
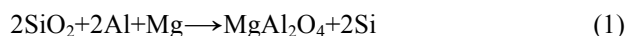


Fig. 3 TEM images of $\text{MgAl}_2\text{O}_4/\text{AC4C-Cu}$ composite

manufactured by crushing larger particles to an average particle size, the particle seemed to have a tendency to fracture along (111) planes. The (113) plane of Al is parallel to the (111) plane of MgAl_2O_4 , but it is not a perfect parallel and there is an angle of about 3° between them. The angle between $(1\bar{1}3)$ plane of MgAl_2O_4 and the interface was about 59° , and the angle between the (111) plane of Al and the interface was about 56° . Because the mismatch between the $(1\bar{1}3)$ plane spacing of MgAl_2O_4 and (111) plane spacing of Al is 4.1%, it is considered that the growth of Al on the (111) plane of MgAl_2O_4 with a cube-on-cube orientation relationship is difficult. However, the mismatch was reduced to about 0.38% due to the (111) plane of Al being shifted about 3° against the interface, and the good lattice matching between the two phases at the interface occurred. Some dislocations were observed in the matrix around the particle resulting from the mismatch of thermal expansion coefficients between MgAl_2O_4 and Al. The density of dislocation was high near the interface, but was lowered while away from the particle.

When the oxidized SiC particles and Al_2O_3 particles were incorporated into Mg-containing aluminum alloy, the MgAl_2O_4 generated from the following two possible reactions [5–10]:



For the oxidized SiC particles, because the thin SiO_2 layer was formed on the surface of SiC particles by oxidation at high temperatures, the reaction between the oxidized SiC particle and Al–Mg was considered to be Eq. (1). According to Eqs. (1) and (2), MgAl_2O_4 particles were formed on the surfaces of SiC and Al_2O_3 particles. Therefore, the microstructures of SiC– MgAl_2O_4 –Al and Al_2O_3 – MgAl_2O_4 –Al would generate in some places on the surfaces of the particles. In addition, when the reactions were intense, a thin layer of MgAl_2O_4 would be formed on the surfaces of SiC and Al_2O_3 particles, and SiC and Al_2O_3 particles were not directly formed at the interfaces with Al on the whole surfaces of the particles. Therefore, the interfaces of SiC– $i_{\text{S-M}}$ – MgAl_2O_4 – $i_{\text{M-Al}}$ –Al and Al_2O_3 – $i_{\text{AO-M}}$ – MgAl_2O_4 – $i_{\text{M-Al}}$ –Al were formed in the composites, where, $i_{\text{S-M}}$ are $i_{\text{AO-M}}$ are the interfaces between the reinforcement particles and MgAl_2O_4 layer, and $i_{\text{M-Al}}$ is the interface between the MgAl_2O_4 layer and Al. The layer or particles of MgAl_2O_4 grew in-situ on the surface of the reinforcement particles, and the bonding strengths at the interfaces of $i_{\text{S-M}}$ and $i_{\text{AO-M}}$ were strong. Therefore, it is obviously that interface between the MgAl_2O_4 and Al ($i_{\text{M-Al}}$) is the most important factor for oxidized SiC and Al_2O_3 particles-reinforced Mg-containing aluminum alloy composites. In the present study, the interface between the MgAl_2O_4 particle and Al was formed directly during the solidification, and it was thought that the bonding strength was strong due to the good lattice matching between the two phases at the interface.

3.3 Tensile strength and fatigue properties

The ultimate tensile strengths of the AC4C based alloys and the MgAl_2O_4 particle-reinforced AC4C based alloy composites after heat treatment at T6 are shown in Table 1. When the average particle size was $2.5 \mu\text{m}$ (referred as fine particle), due to the agglomeration of the particles during the fabrication process, the tensile strength of the composite was lower than that of the matrix alloy, and was 285 MPa. By observing the fracture surfaces of the composite, it was found that the fracture origins of the fine particle-reinforced composite were the flaws caused by the agglomeration of particles. When using the non-classified particles with an average particle size of $12.5 \mu\text{m}$ as reinforcement, the dispersibility of the particles was improved compared with the fine particles, but the tensile strength was about the same as the strength of the matrix alloy. On the other hand, when using the classified particles with an average particle size of $9.6 \mu\text{m}$, the tensile strengths of $\text{MgAl}_2\text{O}_4/\text{AC4C-Mg}$ and $\text{MgAl}_2\text{O}_4/\text{AC4C-Cu}$

composites were 376 MPa and 383 MPa, and were about 5.5% and 3.5% higher than those of matrix alloys, respectively. By excluding the particles with a size below 5 μm via classification process of the particles, the dispersion of the particles was improved, and the tensile strength of the aluminum alloy was increased by incorporating the classified particles into matrix alloys.

Table 1 Tensile strength of aluminum alloys and composites

Materials	Particle size/ μm	Tensile strength/MPa
AC4C–Mg		348
AC4C–Cu		370
MgAl ₂ O _{4p} /AC4C–Mg	2.5	285
MgAl ₂ O _{4p} ^a /AC4C–Mg	12.2	349
MgAl ₂ O _{4p} ^c /AC4C–Mg	9.6	367
MgAl ₂ O _{4p} ^c /AC4C–Cu	9.6	383

Usually, the particle-reinforced composites were fabricated by the stirring–casting method or the powder metallurgy method combined with a secondary process such as forging, extrusion or rolling, and it is found that the tensile strength of the composite increases with decreasing the particle size due to the fact that the following secondary process can be used to break up the stirring induced or the powder mixing induced reinforcement agglomerates, homogenizing their distribution, and eliminating porosity when the average size of the particles was in the range of 3–40 μm [11–13]. However, when using stirring–casting method without a secondary process, the dispersion of the particles would be deteriorated, and the tensile strength of the composites would be lowered when the particle size was below a certain critical size. The critical size of the particle is about 5 μm in this present study, but it is considered to be significantly influenced by the atmosphere during the fabricating, the composition of the alloy, the addition of the wetting element, and the fabrication conditions. By using the classified MgAl₂O₄ particle, though the compositions of the AC4C based alloys were changed, the effects of the reinforcements on the tensile strengths were confirmed in AC4C–Mg and AC4C–Cu alloy composites. However, the reinforcing effect for the AC4C–Mg alloy having a low strength was higher than that for the AC4C–Cu alloy having a high strength as reported elsewhere [14]. The tensile strength of the AC4C–Mg alloy and AC4C–Cu alloy reinforced by the addition of 10% SiC particles were higher than those of the un-reinforced alloys by about 6.9% and 5.7%, respectively [14]. It is obviously that reinforcing effect of the MgAl₂O₄ particle is slightly lower than that of SiC particle. Previously, it was proposed that the strengthening of Al alloys due to the addition of the

ceramic particle reinforcements occurred as the results of the presence of numerous reinforcement/matrix interfaces, the formation of complex, high density dislocation structures in interfacial areas, the development of inter stresses in matrix, and accelerated precipitation kinetics [15–17]. The generation of dislocation was due to a difference in thermal coefficient of expansion between the matrix and the reinforcement particle. Because the thermal expansion coefficient of MgAl₂O₄ particle is greater than that of SiC particle, it is thought that the formation of the plastic zone containing high density dislocation in the matrix around the particle was disadvantageous for MgAl₂O₄ particle, and then the reinforcing effect of MgAl₂O₄ particle was lower than that of the SiC particle.

Cyclic stress amplitude versus the number of cycles to failure at room temperature is shown in Fig. 4. Arrows shown in the figure indicate that the specimens were not broken from the fatigue tests after 10⁷ cycles. The fatigue life of the composite was longer than that of the unreinforced alloy. However, the fatigue life of the composite at high stresses converged with un-reinforced alloy. The fatigue limits at 10⁷ cycles for unreinforced AC4C–Cu alloy and MgAl₂O_{4p}/AC4C–Cu composite were 120 MPa and 135 MPa, respectively. The fatigue strength for the composite increases by 12.5% compared to that for alloy. The optical micrographs of the fracture surface of AC4C–Cu alloy and MgAl₂O_{4p}/AC4C–Cu composite fatigued at stress amplitude of 150 MPa at room temperature are shown in Fig. 5. The fatigue surfaces display the origin of fatigue crack, the region of fatigue crack propagation, and the region of fast fracture. The origins of fatigue cracks were near the surface of specimen. The area of the region of fatigue crack propagation in AC4C–Cu alloy was larger and the surface was greatly undulated. Compared with the fracture surface of AC4C–Cu alloy, the area of the region of

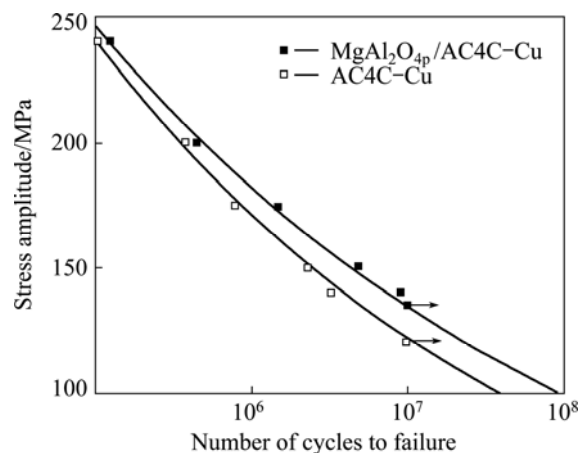


Fig. 4 Stress amplitude versus number of cycles to failure for fatigue of AC4C–Cu alloy and MgAl₂O_{4p}/AC4C–Cu composite at room temperature

fatigue crack propagation in $\text{MgAl}_2\text{O}_4/\text{AC4C-Cu}$ composite was small and the surface was relatively flat. When increasing the stress amplitude, the number of cycles to failure and the area of the region of fatigue crack propagation decreased, and the area of the region of the fast fracture increased. At the same stress amplitude, because the fatigue life of the composite was longer and the area of the region of the fatigue crack propagation was smaller in $\text{MgAl}_2\text{O}_4/\text{AC4C-Cu}$ composite than in AC4C-Cu alloy, it is obvious that MgAl_2O_4 particles had qualities to obstruct the formation and propagation of fatigue cracking.

The SEM micrographs of the fracture surfaces of the $\text{MgAl}_2\text{O}_4/\text{AC4C-Cu}$ composite fatigued at stress amplitude of 150 MPa and 240 MPa at room temperature are shown in Fig. 6. The origins of fatigue cracks were internal flaw and surface flaw, and the sizes of the flaws were about 100 μm . By observing the fracture surfaces, it

was found that most of the internal and surface flaws were the particle agglomeration induced blowholes as shown in Fig. 6. Fatigue cracks initiated and grew from the origin, and then propagated slowly. During the propagation of the fatigue crack, the crack would progress fast when the remaining area of the specimen cannot withstand the load, and fracture catastrophically. Fatigue striations and few MgAl_2O_4 particles were observed in the region of crack propagation. Because the number of MgAl_2O_4 particles observed from the region of crack propagation was much less than the amount of the added particles, it is obvious that MgAl_2O_4 particles and $\text{MgAl}_2\text{O}_4/\text{Al}$ interfaces resisted the failure causing the fatigue cracks to propagate around the particle resulting in extensive crack deflection. Because the particle fracture, de-bonding at the interface and the crack deflection around the reinforcement particles at the region of fatigue crack propagation were influenced by

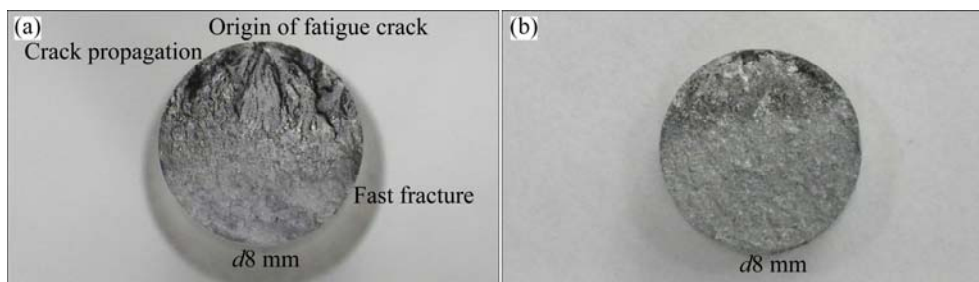


Fig. 5 Fracture surfaces of AC4C-Cu and $\text{MgAl}_2\text{O}_4/\text{AC4C-Cu}$ composite fatigued at stress amplitude of 150 MPa at room temperature: (a) AC4C-Cu , 2.31×10^6 cycles; (b) $\text{MgAl}_2\text{O}_4/\text{AC4C-Cu}$, 4.82×10^6 cycles

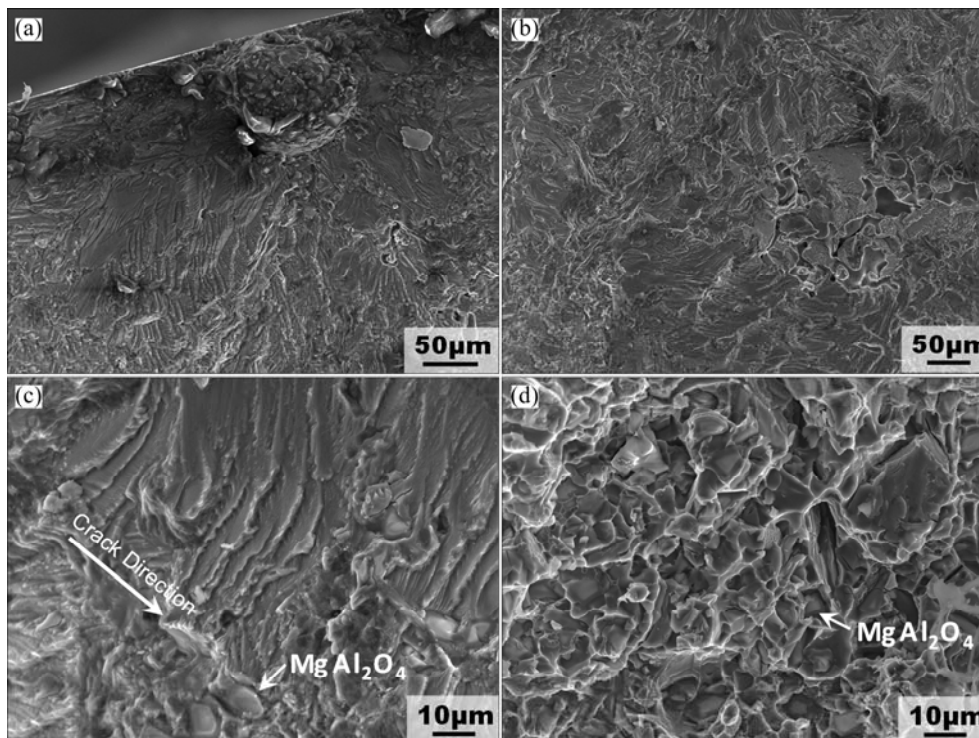


Fig. 6 Fracture surfaces of $\text{MgAl}_2\text{O}_4/\text{AC4C-Cu}$ composite fatigued at stress amplitude of 240 MPa after 1.27×10^5 cycles (a), 150 MPa after 4.82×10^6 cycles (b–d) (same sample with Fig. 4(b)) at room temperature: (a), (b) Near origin of fatigue crack; (c) Striation pattern in region of fatigue crack propagation; (d) Region of fast fracture

the mismatch of the thermal coefficient of expansion between the matrix and the reinforcement particle, almost no SiC particles have been found from this region due to a higher mismatch and higher particle strength in the SiC_p/AC4C–Cu composite compared with the MgAl₂O_{4p}/AC4C–Cu composite [14]. Dimples were observed from the final part of the region of crack propagation and the region of fast fracture, and MgAl₂O₄ and Si particles were observed from the bottoms of the dimples. The micro-dimples were observed from the surfaces of some MgAl₂O₄ particles, indicating strong bonding existing at the interface between the particle and matrix. In the region of fast fracture, the number of MgAl₂O₄ particles observed from the fracture surface was almost the same as the amount of the added particles, and the particles uniformly distributed across the surface. Examination of fracture surfaces of powder metallurgy processed particle-reinforced composites revealed that very few SiC particles were observed from the crack initiation and the particle fractures increased from crack initiation to fast fracture [18,19]. Though the microstructures were different between the powder metallurgy and stirring–casting processed composites, the same phenomenon was observed in the present study. Because MgAl₂O₄ particles were hardly observed from the vicinity of the fatigue crack origin and the region of the fatigue crack propagation, it is believed that de-bonding at the interface between matrix and particles was not generated, fatigue crack propagation was to avoid the MgAl₂O₄ particles due to the high-density dislocation in the matrix near the interface, and the fatigue crack would propagate in the matrix preferentially. The formation of the plastic zone contained high-density dislocation in the matrix due to a thermal expansion mismatch between the MgAl₂O₄ particle and the matrix, resisting the generation and the propagation of the fatigue crack by crack deflection and crack bowing, which contributed to the improvement of fatigue strength.

At 250 °C, the fatigue limits at 10⁷ cycles in the unreinforced AC4C–Cu alloy and MgAl₂O_{4p}/AC4C–Cu composite were 55 and 70 MPa, respectively, as shown in Fig. 7. The fatigue limit at 10⁷ cycles in the MgAl₂O_{4p}/AC4C–Cu composite increased by 27% compared to that for the unreinforced alloy. The strengthening effect of the MgAl₂O₄ particle on the fatigue strength at elevated temperature is much higher than that at room temperature.

The SEM micrographs of the fracture surface of the MgAl₂O_{4p}/AC4C–Cu composite fatigued at stress amplitude of 80 MPa at 250 °C are shown in Fig. 8. The origin of fatigue crack was a surface flaw, and the size of the flaw was about 50 μm. It is found that the size of

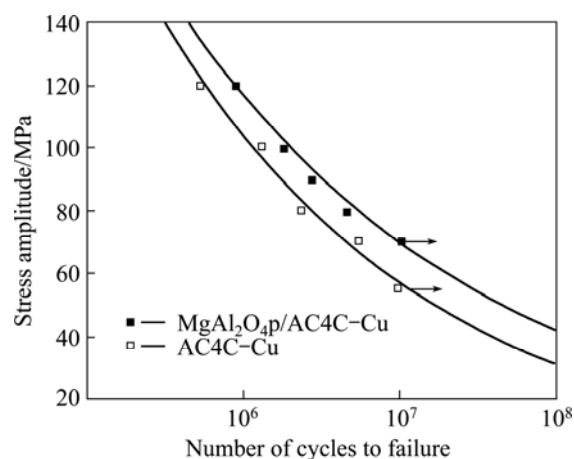


Fig. 7 Stress amplitude versus number of cycles to failure for fatigue of AC4C–Cu alloy and MgAl₂O_{4p}/AC4C–Cu composite at 250 °C

origin of the fatigue crack was smaller at high temperature than at room temperature, and the fatigue crack initiated from a defect in the matrix rather than a defect due to agglomeration of particles in some cases. Particle fractures were not observed from the region of crack propagation, but the fatigue striations were observed as shown in Fig. 8. The fatigue crack initiation sites would change from the intermetallic inclusions and particle clusters at ambient temperature to the matrix at elevated temperatures due to the matrix softening and the creep at high temperature. The load transferred from the matrix to the reinforcements was reduced with the matrix strength, and thus the critical stress for particle fracture was not attained [20,21]. As the fatigue crack approached the region of the fast fracture, the fracture surface transitioned from shear type to tensile type, and finally fractured catastrophically. The morphology of the region of the fast fracture was substantially the same as the fracture surface fatigued at room temperature. A lot of dimples were observed around MgAl₂O₄ particles, and micro-dimples were also observed from the surfaces of some MgAl₂O₄ particles, indicating strong bonding existing at the interface between the particle and matrix. The formation of the plastic zone containing high-density dislocation in the matrix due to the thermal expansion mismatch between the MgAl₂O₄ particle and the matrix, also resisted the generation and the propagation of the fatigue crack by the crack deflection and crack bowing, which contributed to the improvement of fatigue strength at elevated temperatures. It was reported that the fatigue failure of the composite was believed to be caused by a mechanism of nucleation, growth and coalescence of voids in the matrix around the reinforcements at elevated temperatures, and the cavitation damage was dominated by a diffusion-controlled process [20–23]. Because the reinforcing effect of MgAl₂O₄ particles on the fatigue life

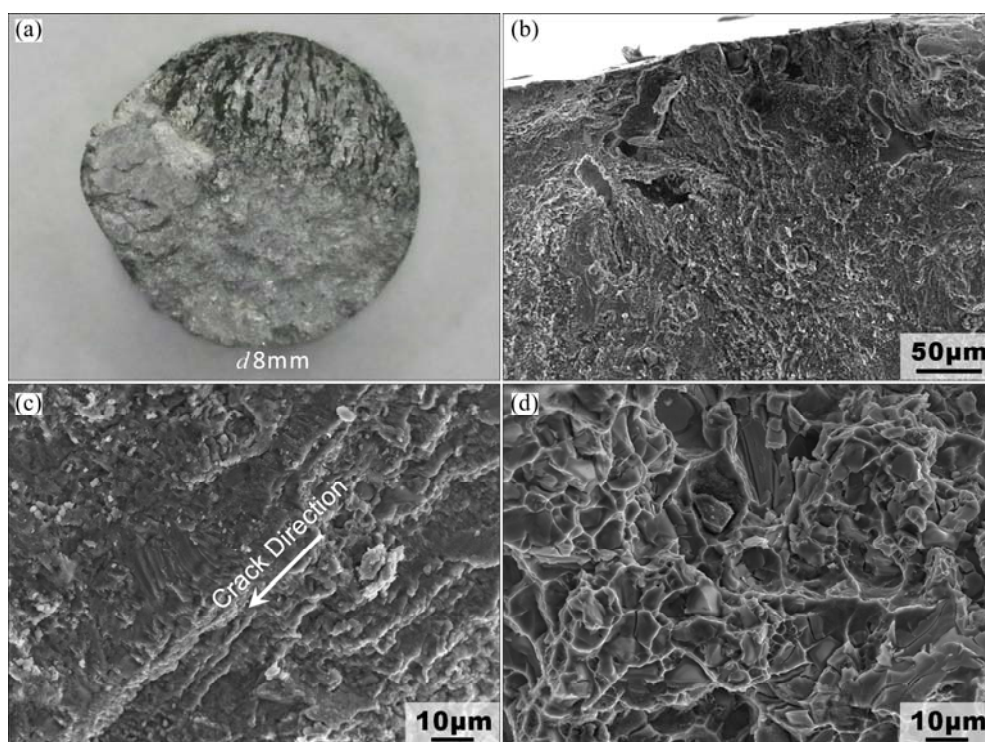


Fig. 8 Fracture surfaces of $\text{MgAl}_2\text{O}_4/\text{AC4C-Cu}$ composite fatigued at stress amplitude of 80 MPa after 4.6×10^6 cycles at 250 °C: (a) Optical micrograph; (b) Near origin of fatigue crack; (c) Striation pattern in region of fatigue crack propagation; (d) Region of fast fracture

at elevated temperatures was almost the same as that of SiC particles, it is considered that the resistance to the matrix softening, the generation of voids, and the creep in the matrix by the particles played more important role in the reinforcing effect of particles at elevated temperatures compared with the formation of high-density dislocation due to the thermal expansion mismatching between the particle and the matrix at room temperature.

4 Conclusions

1) MgAl_2O_4 particle reinforced AC4C based alloy composites were fabricated by the stirring-casting method. In order to improve the dispersibility of the particles, the as-received MgAl_2O_4 particles were classified, and the particles with a size in range of 5–25 μm were collected and used for fabricating the composite. The classified particles were uniformly distributed in the matrix, and the tensile strength of composite increased by using the classified particles.

2) Dislocations were observed in the matrix around the MgAl_2O_4 particle resulting from the mismatch of thermal expansion coefficients between MgAl_2O_4 and Al, and a strong bonding existed at the interface between the MgAl_2O_4 particle and matrix due to the good lattice matching between the two phases.

3) The fatigue limits of $\text{MgAl}_2\text{O}_4/\text{AC4C-Cu}$ composite at room temperature and 250 °C after 10^7 cycles were 135 MPa, and 70 MPa, and increased by 12.5%, and 27% compared the that of the un-reinforced alloy, respectively.

4) The high strength of MgAl_2O_4 particle and the $\text{MgAl}_2\text{O}_4/\text{Al}$ interface, and the formation of the plastic zone containing high-density dislocation in the matrix due to the thermal expansion mismatch between the MgAl_2O_4 particle and the matrix, resisted failure by fatigue cracks to propagate around the MgAl_2O_4 particle, resulting in extensive crack deflection and crack bowing, which contributed to the improvement of fatigue strength at room temperature. But the resistance to the matrix softening, the generation of voids, and the creep in the matrix by the particles played the most important role in the reinforcing effect of particles at elevated temperatures.

References

- [1] ISEKI T, KAMEDA T, MARUYAMA T. Interfacial reactions between SiC and aluminium during joining [J]. *Journal of Materials Science*, 1984, 19(5): 1692–1698.
- [2] SHOROWORDIA K M, LAOUIB T, HASEEBA A S M A, CELISB J P, FROYENB L. Microstructure and interface characteristics of B_4C , SiC and Al_2O_3 reinforced Al matrix composites: a comparative study [J]. *Journal of Materials Processing Technology*, 2003, 142(3): 738–743.

- [3] PECH-CANUL M I, MAKHLOUF M M. Processing of Al–SiC_p metal matrix composites by pressureless infiltration of SiC_p performs [J]. *Journal of Materials Synthesis and Processing*, 2000, 8(1): 35–53.
- [4] YAGHMAEE M S, KAPTAY G. Stability of SiC in Al-rich corner of liquid Al–Si–Mg system [J]. *Materials Science Forum*, 2005, 473–474(1): 415–420.
- [5] ZHON W M, L'ESPERANCE G, SUERYB M. Effect of current Mg concentration on interfacial reactions during remelting of Al–Mg(5083)/Al₂O_{3p} composites [J]. *Materials Characterization*, 2003, 49(2): 113–119.
- [6] ZHOU Z, FAN, Z, PENG H X, LI D X. High-resolution electron microscope observation of interface microstructure of a cast Al–Mg–Si–Bi–Pb(6262)/Al₂O_{3p} composite [J]. *Journal of Microscopy*, 2001, 201(2): 144–152.
- [7] MATSUDA K, MATSUKI T, MULLEROVA I, FRANK L, IKENO S. Morphology of spinels and Al₂O₃ particles in an Al₂O₃/Al–Mg–Si composite material revealed by scanning low energy electron microscopy [J]. *Materials Transaction, JIM*, 2006, 47(7): 1815–1820.
- [8] SHI Z L, YANG J M, LEE J C, ZHANG D, WU R J. The interfacial characterization of oxidized SiC_p/2014 Al composite [J]. *Materials Science and Engineering A*, 2001, 303(1–2): 46–53.
- [9] ZHOU W, XU Z M. Casting of SiC reinforced metal matrix composites [J]. *Journal of Materials Processing Technology*, 1997, 63(1–3): 358–363.
- [10] LUO Z P, SONG Y G, ZHANG S Q. A TEM study of the microstructure of SiC_p/Al composite prepared by pressureless infiltration method [J]. *Scripta Materialia*, 2001, 45(10): 1183–1189.
- [11] HALL J N, JONES J W, SACHDEV A K. Particle size, volume fraction and matrix strength effects on fatigue behavior and particle fracture in 2124 aluminum–SiC_p composites [J]. *Materials Science and Engineering A*, 1994, 183(1–2): 69–80.
- [12] WILLIAMS J J, PIOTROWSKI, SAHA R, CHAWLA N. Effect of overaging and particle size on tensile deformation and fracture of particle-reinforced aluminum matrix composites [J]. *Metallurgical and Materials Transactions A*, 2002, 33(12): 3861–3869.
- [13] HAN N L, WANG Z G, ZHANG G D. Effect of reinforcement size on the elevated-temperature tensile properties and low-cycle fatigue behavior of particulate SiC/Al composites [J]. *Composites Science and Technology*, 1997, 57(11): 1491–1499.
- [14] IIZUKA T, OUYANG Q B. Strengths and fatigue properties of SiC particle-reinforced AC4C based alloy composites fabricated by gravity casting [J]. *Light Metals*, 2013, 63(11): 400–405.
- [15] ARSENAULT R J, WANG L, FENG C R. Strengthening of composites due to microstructural changes in the matrix [J]. *Acta Metall Mater*, 1991, 39(1): 47–57.
- [16] WU Y, LAVERNIA. Strengthening behavior of particulate reinforced MMCs [J]. *Scripta Metallurgica et Materialia*, 1992, 27(2): 173–178.
- [17] MILLER W S, HUMPHREYS F J. Strengthening mechanisms in particulate metal matrix composites [J]. *Scripta Metallurgica et Materialia*, 1991, 25(1): 33–38.
- [18] CHEN Z Z, HE P, CHEN L Q. The role of particles in fatigue crack propagation of aluminum matrix composites and casting aluminum alloys [J]. *J Mater Sci Technol*, 2007, 23(2): 213–216.
- [19] MASON J J, RITCHIE R O. Fatigue crack growth resistance in SiC particulate and whisker reinforced P/M 2124 aluminum matrix composites [J]. *Materials Science and Engineering A*, 1997, 231(1–2): 170–182.
- [20] ZHU S J, IIZUKA T. Fatigue behavior of Al₁₈B₄O₃₃ whisker-framework reinforced Al matrix composites at high temperatures [J]. *Composites Science and Technology*, 2003, 63(2): 265–271.
- [21] LLORCA J. Fatigue of particle-and whisker-reinforced metal-matrix composites [J]. *Progress in Materials Science*, 2002, 47(3): 283–353.
- [22] WANG L, SUN Z M, KOBAYASHI T, TODA H. Cyclic deformation and low cycle fatigue behavior in a SiCw/6061Al composite at elevated temperature [J]. *Materials Transactions, JIM*, 1996, 37(10): 1561–1567.
- [23] SYU D G C, GHOSH A K. The effect of temperature on the fracture mechanism in 2014Al/15vol.%Al₂O₃ composite [J]. *Material Science and Engineering A*, 1994, 184(1–2): 27–35.

MgAl₂O₄ 颗粒增强型 AC4C 基复合材料的 微观组织及力学性能

Tateoki IIZUKA¹, 欧阳求保²

1. Isuzu Advanced Engineering Center, Ltd., Kanagawa 252-0881, Japan;

2. State Key Laboratory of Metal Matrix Composites, Shanghai Jiao Tong University, Shanghai 200240, China

摘要: 采用搅拌铸造方法制造 MgAl₂O₄ 颗粒增强型 AC4C 基复合材料。考察 MgAl₂O₄ 颗粒的尺寸及尺寸分布对颗粒分散度的影响, 并且测试复合材料的微观组织、强度与疲劳性能。5~25 μm 范围内的 MgAl₂O₄ 颗粒可以提高复合材料的抗拉强度。疲劳性能测试表明, 在 250 °C、10⁷ 循环周期内, MgAl₂O₄ 颗粒使复合材料的疲劳性能提高 27%。在 MgAl₂O₄ 颗粒周围, 观察到了大量位错, 产生这种情况的主要原因是 MgAl₂O₄ 与 Al 两者之间的热膨胀系数不匹配。在 MgAl₂O₄ 颗粒周围产生裂纹, 但在扩展过程中大量的裂纹发生了转向和弯曲, 这有助于材料疲劳性能的提高。

关键词: MgAl₂O₄ 颗粒; AC4C 铝基; 颗粒的分类; 复合; 疲劳; 抗拉强度

(Edited by Hua YANG)